Apoptosis in podocytes induced by TGF-β and Smad7

Mario Schiffer,[1] Markus Bitzer,[1] Ian S.D. Roberts,[2] Jeffrey B. Kopp,[3] Peter ten Dijke,[4] Peter Mundel,[1,5] and Erwin P. Böttinger[1,6]

[1]Division of Nephrology, Department of Medicine, Albert Einstein College of Medicine, Bronx, New York, USA
[2]Department of Pathological Sciences, The University of Manchester, Manchester, United Kingdom
[3]Kidney Disease Branch, National Institute of Diabetes, Digestive and Kidney Disease, NIH, Bethesda, Maryland, USA
[4]Division of Cellular Biochemistry, The Netherlands Cancer Institute, Amsterdam, The Netherlands
[5]Department of Anatomy and Structural Biology, and
[6]Department of Molecular Genetics, Albert Einstein College of Medicine, Bronx, New York, USA

Address correspondence to: Erwin P. Böttinger, Albert Einstein College of Medicine, 1300 Morris Park Avenue, Bronx, New York 10461, USA. Phone: (718) 430-3158; Fax: (718) 430-8963; E-mail: bottinge@aecom.yu.edu.

Mario Schiffer and Markus Bitzer contributed equally to this work.

Primary and secondary forms of focal segmental glomerulosclerosis (FSGS) are characterized by depletion of podocytes and constitute a central manifestation of chronic progressive glomerular diseases. Here we report that podocytes undergo apoptosis at early stages in the course of progressive glomerulosclerosis in TGF-β1 transgenic mice. Apoptosis is associated with progressive depletion of podocytes and precedes mesangial expansion. Smad7 protein expression is strongly induced specifically in damaged podocytes of transgenic mice and in cultured murine podocytes treated with TGF-β. TGF-β1 and Smad7 each induce apoptosis in podocytes, and their coexpression has an additive effect. Activation of p38 MAP kinase and caspase-3 is required for TGF-β–mediated apoptosis, but not for apoptosis induced by Smad7. Unlike TGF-β, Smad7 inhibits nuclear translocation and transcriptional activity of the cell survival factor NF-κB. Our results suggest a novel functional role for Smad7 as amplifier of TGF-β–induced apoptosis in podocytes and a new pathomechanism for podocyte depletion in progressive glomerulosclerosis.

J. Clin. Invest. **108**:807–816 (2001). DOI:10.1172/JCI200112367.

Introduction

Primary or secondary focal segmental glomerulosclerosis (FSGS) with tubulointerstitial fibrosis is a common feature in chronic progressive renal disease (1). Injury and depletion of glomerular podocytes, leading to podocyte "insufficiency" and capillary collapse, have been invoked as important steps in the development of FSGS (2, 3).

Podocytes are highly specialized cells characterized by actin-rich foot processes that reside on the glomerular basement membrane (GBM). These cells have a critical role in the maintenance of structure and function of the glomerular filter. Injury to the glomerulus is usually characterized by disappearance or effacement of foot processes leading to leakage of protein into the urine (proteinuria). In many cases of nephrotic syndrome in children, and most adult renal diseases associated with proteinuria, foot process effacement is considered an early manifestation in a continuum of progressive podocyte damage characterized by vacuolization, pseudocyst formation, detachment of podocytes from the GBM and, finally, irreversible loss of podocytes (4). Although these observations suggest that cellular damage and loss of podocytes may be an important, initial event in the irreversible progression of glomerulosclerosis, the underlying molecular pathomechanisms remain poorly understood.

TGF-β is a pleiotropic cytokine that accumulates in injured kidneys in experimental animal models and virtually every type of chronic renal disease in humans (5). Smad family proteins include both positive and negative mediators of TGF-β signaling (6). Smad7 has been identified as a negative regulator of TGF-β/SMAD signaling that is responsive to TGF-β itself, presumably as part of an autoinhibitory feedback loop (7), and to factors known to antagonize TGF-β's activities, including TNF-α and IFN-γ (8). Although exaggerated TGF-β signaling is considered a major profibrotic stimulus in mesangial injury and expansion, little is known about its pathobiology in podocytes.

In this report, we demonstrate that podocytes undergo apoptosis associated with marked upregulation of Smad7 expression at early stages in the course of progressive glomerulosclerosis in TGF-β1 transgenic (TG) mice. Both TGF-β1 and expression of Smad7 promote apoptosis in cultured podocytes through different mechanisms. TGF-β induces apoptosis by activation of mitogen-activated protein (MAP) kinase p38 and classic effector caspase-3, whereas TGF-β–inducible Smad7 inhibits signaling by the cell survival factor NF-κB, resulting in amplification of TGF-β–mediated apoptosis in podocytes.

Methods

TG mice

Albumin/TGF-β1 TG mice have been described previously (9). Blood was collected by retroorbital puncture, from 2- and 5-week-old mice, and serum and urine chemistries were examined as described elsewhere (9). Kidney tissue was fixed by overnight immersion in formaldehyde and paraffin-embedded for histological examination, or snap-frozen in liquid nitrogen for RNA extraction as described.

Cell culture

Cultivation of conditionally immortalized mouse podocytes was performed as reported previously (10). To propagate podocytes, cells were cultivated on type I collagen at 33°C in the presence of 20 U/ml mouse recombinant IFN-γ (Sigma Chemical Co., St. Louis, Missouri, USA) to enhance expression of a thermosensitive T antigen. To induce differentiation, podocytes were maintained at 37°C without IFN-γ for 14 days.

RNA analysis

RNA was isolated from mouse tissues by guanidinium isothiocyanate extraction and column purification using the RNeasy kit (QIAGEN Inc., Valencia, California, USA). For Northern blot analysis, RNA was electrophoresed on 1% agarose gels and transferred to a filter. Filters were then hybridized with ^{32}P-labeled cDNA probes for mouse Smad7 and GAPDH.

Immunofluorescence labeling

Primary antibodies specific for the following proteins were used: monoclonal mouse anti-synaptopodin (11), affinity-purified rabbit anti-Smad7 antibody (12), monoclonal mouse anti-Smad2 antibody (Transduction Laboratories, Lexington, Kentucky, USA), monoclonal mouse anti-smooth muscle actin (Boehringer Mannheim, Philadelphia, Pennsylvania, USA), and anti-p65 (Biomol Research Laboratories, Plymouth Meeting, Pennsylvania, USA). 4',6-Diamidino-2-phenylindole (DAPI) was used as fluorescent groove binding probe to DNA (Sigma Chemical Co.).

Immunofluorescence labelings were performed as described previously (8, 10). For detection of nuclear morphology, cells were fixed in 4% paraformaldehyde, stained for 10 minutes with DAPI (1 μg/ml), and analyzed via fluorescence microscopy to assess chromatin condensation and segregation.

Morphometry

Digital images were captured using a digital CCD-camera system (Diagnostic Instruments Inc., Sterling Heights, Michigan, USA), connected to a Nikon Inc. microscope (Melville, New York, USA), before morphometric analysis. Sections (3 μm) were immunoperoxidase-labeled for Smad7 and counterstained with hematoxylin and periodic acid-Schiff (PAS) stain. Cells were counted as podocytes if they resided on the outer aspect (urinary space) of PAS-positive basement membrane. Nuclei of cells that resided in areas circumscribed by PAS-positive basement membrane were counted as endocapillary/mesangial cells. Results from all animals in each group were combined for comparative statistical analysis. A total of 180 glomerular profiles were evaluated in each age group of TG mice (n = 6 both for 2-week-old and for 5-week-old TG mice), and 120 in each group of wild-type (WT) mice (n = 4 for both age groups).

Histopathology scoring

Glomerulosclerosis. At least 30 glomeruli per kidney were evaluated by a renal pathologist (I.S.D. Roberts). Segmental glomerulosclerosis or global glomerulosclerosis was considered present if segmental or global increases in glomerular matrix, segmental or global collapse and obliteration of capillary lumina, accumulation of hyaline, and synechial attachments of glomerular tuft and Bowman's capsule were observed in a glomerulus. Segmental glomerulosclerosis and global glomerulosclerosis were scored as percentage of glomeruli with sclerosis relative to all glomeruli examined per mouse. Tubulointerstitial damage was not evaluated in this study.

Podocyte damage (injury). To estimate the extent of damage in podocytes, we examined glomerular profiles for evidence of pseudocyst formation and detachment of podocytes from GBM (2, 4).

Apoptosis detection

For in situ detection of DNA fragmentation, the ApoTag TUNEL assay was used following the manufacturer's protocol (Intergen Co., Purchase, New York, USA).

To detect DNA fragmentation on agarose gel electrophoresis, adherent and floating cells were collected and lysed in lysis buffer with proteinase K. DNA was extracted from digested cells using phenol/chloroform/isoamyl alcohol extraction and isopropanol precipitation and was subjected to electrophoresis on 1.8% agarose gels.

Western blotting

To detect Flag-Smad7 expression, caspase activation, and cleavage of nuclear poly (ADP-ribose) polymerase (PARP), adherent and floating cells were lysed and subjected to 8%–12% SDS-PAGE before transfer to PVDF membranes (NEN Life Science Products Inc., Boston, Massachusetts, USA). Western blotting was performed as described previously (8), using the following primary antibodies: monoclonal anti-Flag M2, polyclonal rabbit anti–caspase-3 (both, Santa Cruz Biotechnology Inc., Santa Cruz, California, USA), anti-Bax (BD PharMingen, San Diego, California, USA), and monoclonal anti-PARP (Enzyme Systems Products Inc., Livermore, California, USA), and using GDP dissociation inhibitor to control for protein loading (GDI; kind gift from P. Scherer, Albert Einstein College of Medicine). Bound primary antibodies were detected with horse-

	Animals	BUN	Albuminuria	Glomerulosclerosis scores (No. of animals per group)			
	(*n*)	(mg/dl)	(Uprot/crea)	0	< 25%	25%–50%	>50%
WT	8	11.9 (range, 8–14)	10.9 (range, 4.1–20.0)	8	–	–	–
TG 2 wk	6	ND	ND	–	–	5	1
TG 5 wk	6	42.3[A] (range, 20–77)	31.5[A] (range, 5.3 to 67.9)	–	–	1	5

Functional and histopathological parameters in WT C57BL/6XCBA mice (2-week-old and 5-week-old mice, *n* = 4 per age group), and 2-week-old and 5-week-old TG mice. BUN is shown as average level. Albuminuria is shown as average ratio of spot protein and creatinine concentrations in urine samples (Uprot/crea). Glomerulosclerosis scores show number of animals per scoring group with 0, <25%, 25–50%, or >50% of glomeruli with segmental or global glomerulosclerosis. [A]$P < 0.05$ for WT compared with 5-week-old TG mice by Student's *t* test. ND, values not determined.

radish peroxidase–labeled anti-mouse and anti-rabbit secondary antibodies, respectively, and visualized with enhanced chemiluminescence reagents (Pierce Chemical Co., Rockford, Illinois, USA).

Adenoviral gene transfer

The adenoviruses encoding LacZ (AdLacZ) and Smad7 (AdSmad7) are described by Fujii et al. (13). Infection conditions for podocytes were optimized following recommendations as described (13). Cells were seeded at densities of 5×10^4 cells/cm² in 100-mm dishes on the day before infection with the indicated moi for 12 hours.

Transfections and luciferase assays

Podocytes were transiently cotransfected with a pSmad7 expression construct or the empty expression vector pcDNA3 together with NF-κB-Luc, a luciferase reporter gene driven by three NF-κB binding sites (14), and a β-galactosidase expression vector pRSV-β-gal using Effectene reagent (QIAGEN). Luciferase and β-galactosidase activities in cell lysates were measured and normalized for transfection efficiency as described previously (8). For indirect immunofluorescence assays, cotransfections were performed with pcDNA3 or pSmad7, together with pEGFP, a green fluorescent protein expression plasmid (CLONTECH Laboratories Inc., Palo Alto, California, USA). Immunofluorescence labeling of podocytes was performed as described elsewhere (8). Cells were maintained without IFN-γ before and after transfection. Recombinant mouse TNF-α (10 ng/ml; Boehringer Mannheim Biochemicals Inc., Indianapolis, Indiana, USA) was applied to transfected cultures 36 hours after transfection.

Results

TGF-β1 TG mice: a murine model to investigate mechanisms of progression of glomerulosclerosis in the kidney. Albumin/TGF-β1 TG mice are characterized by progressive renal disease induced by elevated circulating TGF-β1 (9). Circulating TGF-β1 levels are elevated at 2–3 weeks of age in TG mice and lead to progressive glomerulosclerosis and interstitial fibrosis with renal failure and death in approximately half of TG animals at 5–12 weeks of age.

To define phenotypic characteristics at early and advanced stages of glomerulosclerosis in this model, we examined six 2-week-old and six 5-week-old TG mice

derived from multiple litters. As controls, we examined four 2-week- and four 5-week-old WT control mice. Glomerular pathology resembling glomerulosclerosis was detected in less than half of the examined glomeruli of 2-week-old TG mice (Table 1). At 5 weeks of age, TG mice had developed significant azotemia and albuminuria associated with global glomerulosclerosis with or without segmental accentuation in all glomeruli (Table 1). Glomeruli were normal in all WT mice. These results
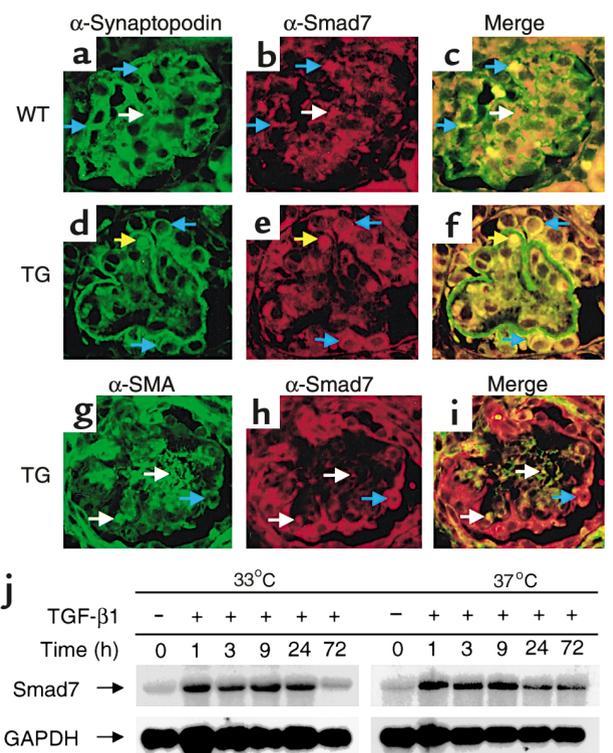
Figure 1
(**a**–**f**) Indirect immunofluorescence of mouse renal cortex sections. Mouse anti-synaptopodin staining (**a** and **d**) visualized with FITC-conjugated anti-mouse IgG; rabbit anti-Smad7 (**b** and **e**) visualized with Cy3-conjugated anti-rabbit IgG in 2-week-old WT (**a**–**c**) and TG mice (**d**–**f**). Podocytes, blue arrows; endocapillary/mesangial cells, white arrows; artifact (red blood cell), yellow arrows. (**g**–**i**) Mouse anti-smooth muscle actin (α-SMA) IgG labeling (**g**) and anti-Smad7 staining (**h**). (**j**) Northern blot shows Smad7 mRNA levels after TGF-β treatment in podocytes cultured under permissive (33°C) or nonpermissive (37°C) conditions. GAPDH is shown for loading control.
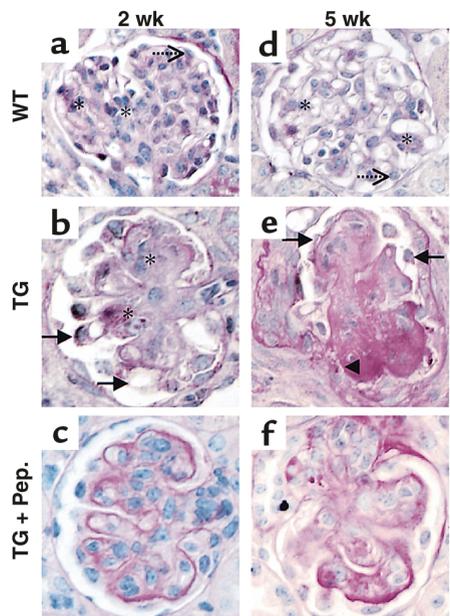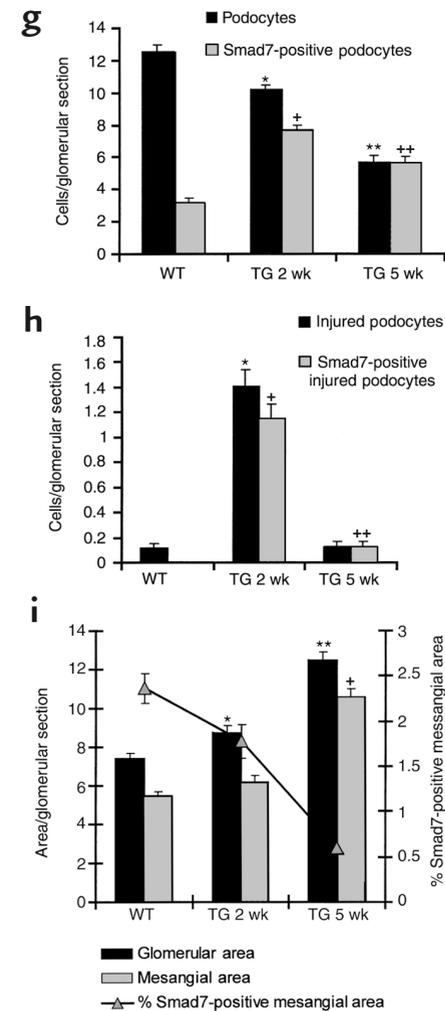
Figure 2

(**a**–**f**) PAS staining and anti-Smad7 immunoperoxidase labeling of renal cortex sections of WT (**a** and **d**) and TG mice (**b** and **e**) at 2 weeks (TG 2 wk) (**a**–**c**) and 5 weeks (TG 5 wk) (**d**–**f**) of age. Absence of Smad7 immunoperoxidase labeling in the presence of blocking peptide in 2-week-old (**c**) and 5-week-old (**f**) TG mice as control for specificity of staining. Dotted arrows depict Smad7-negative podocytes and stars denote Smad7-positive mesangial areas (**a** and **d**). Arrows indicate Smad7-positive podocytes with representative features of damage, including pseudocyst formation and partial or complete detachment from basement membrane (**b** and **e**). Arrowhead shows synechiae of basement membrane and Bowman's capsule (**e**). (**g**) Histogram shows average numbers of podocytes (filled bars) and Smad7-positive podocytes (hatched bars) per central glomerular section. Bars represent average ± SEM numbers of cells per glomerular section determined from 180 glomeruli (30 per mouse) in TGF-β1 TG mice at 2 weeks and at 5 weeks of age, respectively, and 240 glomeruli (30 per mouse) in the WT. Results of t test: *Podocyte counts in WT vs. TG 2 wk, $P < 0.001$; +Smad7-positive podocyte counts in WT vs. TG 2 wk; **podocyte counts in WT vs. TG 5 wk, $P < 0.001$; ++Smad7-positive podocyte counts in WT vs. TG 5 wk, $P < 0.001$. (**h**) Histogram shows numbers of podocytes with criteria of injury (filled bars) and Smad7-positive injured podocytes (hatched bars). Annotations are as described in **g**. (**i**) Histogram shows glomerular surface area (filled bars) and mesangial surface area (hatched bars) per glomerular section in arbitrary units (annotations as in **g**). Line graph indicates ratio of Smad7-positive mesangial area to total mesangial area (see Methods for definitions).

confirm that glomerular lesions typically identified at 2 weeks of age are representative of an early stage, and those typically identified at 5 weeks of age are representative of advanced stages, in the course of progressive glomerulosclerosis caused by TGF-β1 in TG mice.

Expression of Smad7 is upregulated in podocytes and decreased in the mesangium in TGF-β1 TG mice. We observed previously that whole kidney mRNA levels of inhibitory Smad7 were elevated in TG mice with moderate glomerulosclerosis and interstitial fibrosis (M. Schiffer and E. Böttinger, unpublished observations). To determine the glomerular cell type(s) associated with increased Smad7 expression, we performed immunofluorescence double labeling on renal cortex sections. Smad7 protein was expressed predominantly in endocapillary/mesangial areas in WT kidney, whereas only few of the podocytes per section were labeled by Smad7 antibody (Figure 1, a–c). In contrast, most podocyte cell bodies were strongly labeled by Smad7 antibody, whereas only few endocapillary/mesangial cells expressed Smad7 protein in 2-week-old TG mice (Figure 1, d–f). Our data suggest that Smad7 protein expression is induced in podocytes in 2-week-old TG mice, whereas endocapillary/mesangial expression of Smad7, normally observed in WT mice, is decreased in TG mice at this age.

To examine whether TGF-β1 activates Smad7 synthesis in podocytes, we used a conditionally immortalized murine podocyte cell line (10). TGF-β1 rapidly induced Smad7 mRNA levels in podocytes, as has been shown previously in other cell types (15) (Figure 1j). Immunoblots for Smad7 protein showed similar results (data not shown).

Smad7 expression coincides with podocyte damage at an early stage of glomerulosclerosis and is associated with progressive podocyte depletion in TGF-β1 TG mice. To establish semiquantitative measurements of podocyte damage and podocyte numbers and to examine associations with Smad7 expression, we devised a staining strategy combining PAS staining with immunoperoxidase staining for Smad7. Criteria for podocyte damage included pseudocyst formation and partial or complete detachment from basement membrane. Representative glomerular sections in each category are shown in Figure 2. Results are summarized in Table 2.

Average counts of podocytes per glomerular section were not significantly different between 2-week-old and 5-week-old WT mice, but were significantly reduced in 2-week-old TG compared with WT mice, and were further reduced in 5-week-old TG mice (Table 2). Counts of Smad7-positive podocytes were significantly increased in 2-week-old TG compared with WT mice. In 5-week-old TG mice, all podocytes were expressing Smad7. Average counts of damaged podocytes were 14-fold increased in 2-week-old TG compared with WT mice, but not significantly different from age-matched WT mice in 5-week-old TG mice (Table 2). Nearly all damaged podocytes expressed Smad7 in 2-week-old and 5-week-old TG mice. Our results demonstrate that morphological signs of cellular damage are detectable in podocytes at early stages of progressive glomerulosclerosis and are associated with Smad7 protein synthesis in these cells.

Mesangial expansion manifests at an advanced stage of glomerulosclerosis and is associated with loss of Smad7 expression. Given that podocyte damage was apparent at early stages in our model, we wanted to determine whether it was coincident with, or preceded, mesangial expansion. We used NIH Image analysis software (version 6.1; NIH, Bethesda, Maryland, USA) to compute total glomerular section surface area and mesangial section surface area by outlining entire glomerular tuft, or mesangial segments minus capillary lumen of glomerular tufts. Aver-

age glomerular area in arbitrary units was not significantly different between 2-week-old and 5-week-old WT mice, but was increased in 2-week-old TG compared with WT mice, and was further increased in 5-week-old TG mice (Table 2). Average mesangial area per glomerular section was not significantly different between 2-week-old and 5-week-old WT mice or 2-week-old TG mice, but was considerably increased in 5-week-old TG mice (Table 2). These data indicate that mesangial expansion manifests itself during advanced stages of glomerulosclerosis in TG mice. To estimate the extent of Smad7 expression in mesangial areas in TG and WT mice, we determined immunoperoxidase-stained mesangial areas as a fraction of total mesangial area on each examined glomerular section. By this measure, the fractions of Smad7-positive mesangial areas were significantly reduced in both, 2-week-old and 5-week-old TG mice when compared with WT mice (Table 2).

Apoptosis is increased at early stages of progressive glomerulosclerosis in podocytes and at advanced stages in other glomerular cells in TGF-β1 TG mice. To begin to explore the underlying mechanisms of podocyte damage and depletion in our model, we determined rates of apoptosis in podocytes and endocapillary/mesangial cells in WT and TG mice. Podocytes were scored as apoptotic if nuclear labeling by DAPI (blue), cytoplasmic synaptopodin labeling (red), and nuclear TUNEL labeling (green) resulted in turquoise nuclei with red rim (Figure 3, a–l, blue arrows). Overlap of DAPI labeling and TUNEL labeling in the absence of synaptopodin labeling was scored as apoptotic glomerular cells other than podocytes (Figure 3, a–l, white arrows). Colocalizations of synaptopodin labeling and TUNEL staining in the absence of DAPI labeling resulted in yellow signals and were caused by artifactual staining of red blood cells (Figure 3, a–l, yellow arrows). There was a 20-fold increase in the average of TUNEL positive podocytes per glomerular section in 2-week-old TG mice compared with WT, and a fourfold increase in 5-week-old TG mice

Table 2
Summary of analyses of cell counts and surface areas in glomerular sections

	Two-week-old WT	Five-week-old WT	Two-week-old TG	Five-week-old TG
Podocytes per glomerular section				
Total	13.5 ± 3.0	11.6 ± 3.8[A]	10.2 ± 2.7[B]	5.7 ± 2.8[B]
Smad7-positive	2.6 ± 1.4	3.1 ± 1.5[A]	7.4 ± 2.7[B]	5.6 ± 2.2[B]
Damaged	0.1 ± 0.05	0.1 ± 0.07[A]	1.4 ± 0.2[B]	0.2 ± 0.23[A]
Smad7-positive damaged	0	0	1.2 ± 0.2	0.2 ± 0.08
Section surface area (U)				
Glomerular	7.1 ± 2.4	7.6 ± 2.5	8.7 ± 0.4[C]	12.4 ± 0.4[B]
Mesangial	5.1 ± 1.9	5.8 ± 2.0[A]	6.2 ± 0.3[A]	10.6 ± 0.4[B]
%Smad7-pos. mesangial	2.6 ± 1.2	2.1 ± 1.7[A]	1.8 ± 0.2[C]	0.6 ± 0.06[B]
Apoptotic cells per glomerular section				
Podocytes	0.05 ± 0.03	0.06 ± 0.2[A]	0.8 ± 0.2[B]	0.2 ± 0.05[B]
Endocapillary/mesangial	0.2 ± 0.04	0.2 ± 0.1	0.3 ± 0.09[A]	1.1 ± 0.2[C]

[A]Not significant, [B]*P* < 0.001, and [C]*P* < 0.05 compared with 2-week-old WT.
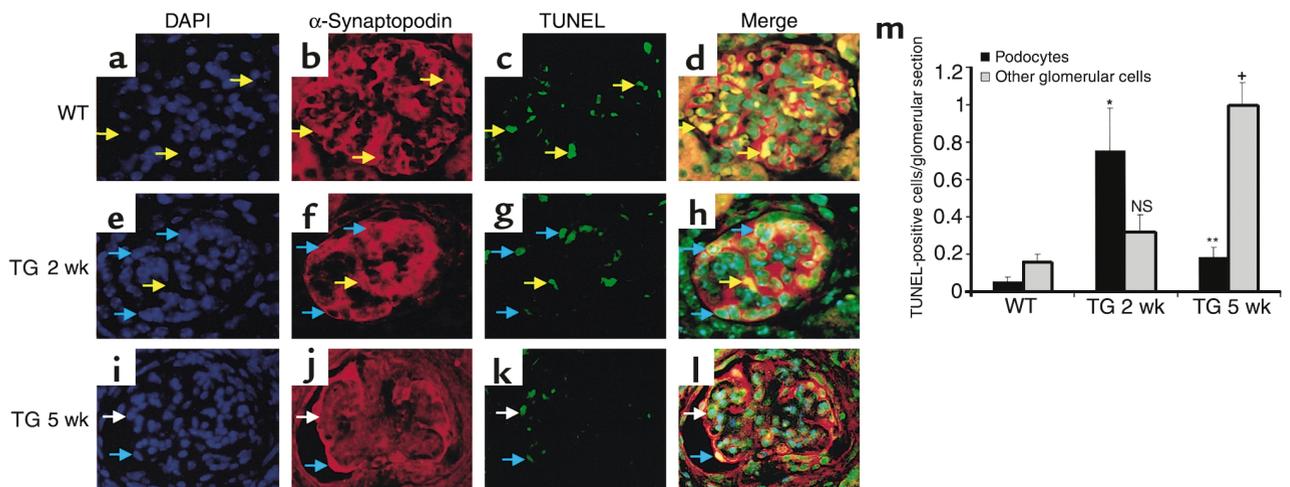
Figure 3

(**a**–**l**) Triple fluorescence labeling using DAPI (**a**, **e**, and **i**), rabbit anti-synaptopodin IgG (**b**, **f**, and **j**), and TUNEL assay (**c**, **g**, and **k**) in renal cortex sections of WT (**a**–**d**), 2-week-old TG (**e**–**h**), and 5-week-old TG (**i**–**l**) mice. TUNEL-positive and DAPI-negative red blood cells (artifacts), yellow arrows; TUNEL-positive podocytes, blue arrows; TUNEL-positive endocapillary/mesangial cells, white arrows. Representative results are shown. (**m**) Average ± SEM of TUNEL-positive podocytes (black bars) and TUNEL-positive endocapillary/mesangial cells (gray bars) per glomerular section. Data for 2-week-old and 5-week old TG are combined. *TUNEL-positive podocytes in WT vs. 2-week-old TG, $P < 0.001$. **Podocytes in WT vs. 5-week-old TG, $P < 0.05$. +Endocapillary/mesangial cells in WT vs. 5-week-old TG, $P < 0.01$. NS, not significant.

(Table 2; Figure 3m). Rates of apoptosis in endocapillary/mesangial cells were not significantly different between WT and 2-week-old TG mice, but were sixfold increased in 5-week-old TG mice. These results demonstrate that increased rates of apoptosis in podoctyes were characteristic for early stages of glomerulosclerosis in this model, and coincided with increased rates of damage in podocytes as determined by morphological criteria (see Figure 2). In contrast, rates of apoptosis in endocapillary/mesangial cells were significantly increased at advanced stages of glomerulosclerosis.

TGF-β1–induced apoptosis in podocytes is associated with increased Bax protein synthesis and caspase-3 activity. We used a conditionally immortalized murine podocyte cell line (10) to explore molecular mechanisms of podocyte apoptosis. Podocytes maintained in both permissive and nonpermissive culture conditions were incubated with TGF-β1 for 2 days before DAPI and TUNEL staining. Podocytes with characteristic morphological features of apoptosis, including condensed nuclei and/or fragmented nuclei (16), and TUNEL-positive nuclei were significantly more common in TGF-β–treated compared with untreated podocytes, irrespective of culture conditions (Figure 4a). TGF-β induced characteristic DNA-fragmentation as early as 24 hours after treatment (Figure 4b). Addition of an inhibitor of caspase-3, Z-Val-Ala-Asp(Ome)-FMK (zVAD-fmk), prevented DNA-fragmentation induced by TGF-β1 (Figure 4b), indicating that TGF-β1 caused apoptosis through activation of effector caspases.

To examine further potential mediators of TGF-β1–induced apoptosis, we analyzed the abundance of Bcl-2 family proteins (Bcl-2, Bcl-X[L], Bad and Bax) and of procaspase-3 by Western blot analysis. Proapoptotic

Bcl2-associated X protein (Bax) expression was increased at 2– 6 hours, followed by a decrease in procaspase-3 levels at 6–48 hours of TGF-β treatment. Induction of caspase-3 activity by TGF-β was confirmed using a fluorimetric assay (Figure 5c). Levels of intact 113-kDa PARP, a substrate of activated caspases, were decreased at 24 and 48 hours, coincident with the appearance of 85-kDa PARP cleavage products (Figure 4c). Together, these data suggest that TGF-β induces apoptosis in podocytes through increased synthesis of the proapoptotic protein Bax and activation of effector caspase-3.

Increased expression of Smad7 is sufficient to induce apoptosis in podocytes through caspase-3–independent pathways. Because we showed that Smad7 expression was increased in injured podocytes in situ in TGF-β TG mice, and that TGF-β stimulated Smad7 synthesis in podocyte cultures, we examined whether Smad7 is able to increase apoptosis in podocytes independently of TGF-β. We used an adenoviral expression system for flag-epitope–tagged Smad7 (AdSmad7) (13) to achieve efficient expression of Flag-Smad7 in infected podocytes, as verified by immunoblotting (Figure 5a) and by indirect immunofluorescence demonstrating infection efficiencies of more than 98% without detectable cellular toxicity at moi's of 100–200 (data not shown). Cellular toxicity and apoptosis were observed at higher moi. Enhanced expression of Smad7 resulted in significantly increased rates of apoptotic nuclei in AdSmad7-infected podocytes, when compared with AdLacZ control infection (Figure 5b). Caspase-3 inhibitor zVAD-fmk had no effect on increased apoptotic rates induced by Smad7 expression, but significantly inhibited TGF-β–mediated increase in apoptotic rates. The proapoptotic effects of Smad7 expression and

of TGF-β were additive (Figure 5b). To verify these results, we used a fluorimetric assay that measures caspase-3 activity (17). Although TGF-β treatment of podocytes significantly increased caspase-3 activity, Smad7 expression had no effect on baseline activity of caspase-3 (Figure 5c). In contrast with TGF-β (see Figure 4c), Smad7 expression had no effect on Bax and pro–caspase-3 protein levels (data not shown). To examine whether the proapoptotic activity of Smad7 required autocrine/paracrine activation of TGF-β, we repeated experiments for quantitation of apoptotic rates in podocyte cultures in the presence of a neutralizing mAb (2G7) against all three TGF-β isoforms (18). Presence of neutralizing anti–TGF-β antibody had no effect on Smad7-mediated apoptosis, but completely inhibited TGF-β–induced apoptosis in podocytes (Figure 5d). Together, these results demonstrate that Smad7 expression potentiates apoptosis in podocytes through caspase-3–independent and TGF-β–independent mechanisms, whereas TGF-β induces apoptosis in podocytes through activation of effector caspase-3. These results are also consistent with the additive proapoptotic effects of Smad7 and TGF-β1 in podocytes (Figure 5b).

MAP kinase p38 signaling is required for induction of apoptosis by TGF-β, but not by Smad7. Because we demonstrated that Smad7 expression inhibits Smad3/4-dependent transcriptional activation of reporter genes by TGF-β (M. Schiffer and E. Böttinger, unpublished data) whereas it augments TGF-β–induced apoptosis in podocytes, we examined whether Smad-independent signal transducers including proapoptotic p38 MAP kinase were required for the apoptotic response.

Immunoblot analysis using monoclonal anti-phospho-p38 antibody confirmed activation of p38 MAP kinase by TGF-β after 20 minutes of treatment (Figure 6a). In contrast, we were unable to detect an effect of Smad7 expression on p38 phosphorylation in transduced podocytes (data not shown). Next, we repeated experiments to quantitate Smad7- and TGF-β–induced apoptosis in podocytes in the absence or presence of a chemical inhibitor of p38 (SB203580). SB203580 had no effect on apoptosis induced by Smad7 expression, although it blocked TGF-β–induced apoptosis completely (Figure 6b). These results suggest that MAP kinase p38 signaling is required for induction of apoptosis by TGF-β, but not by Smad7, in podocytes.

Smad7 expression in podocytes inhibits basal and inducible nuclear translocation and transcriptional activator function of anti-apoptotic survival factor NF-κB/p65. NF-κB/p65 is a signal transducer/transcriptional activator complex with well-established functional roles as anti-apoptotic cell survival factor (19). Recent reports indicate that inhibition of NF-κB/p65 causes spontaneous apoptosis independent of caspase activity in lymphoblastoid cells (20) and also suggest a potential role for Smad7 in inhibition of NF-κB (21). Thus, we reasoned that Smad7 may stimulate apoptosis in podocytes by blocking NF-κB/p65 activity. Podocytes were transiently cotransfected with green-fluorescent protein vector pEGFP together with either pcDNA3 control or pSmad7 expression vectors. Immunofluorescence analysis using anti-p65 antibody demonstrated that nuclear p65 labeling was significantly reduced in pSmad7-transfected podocytes at
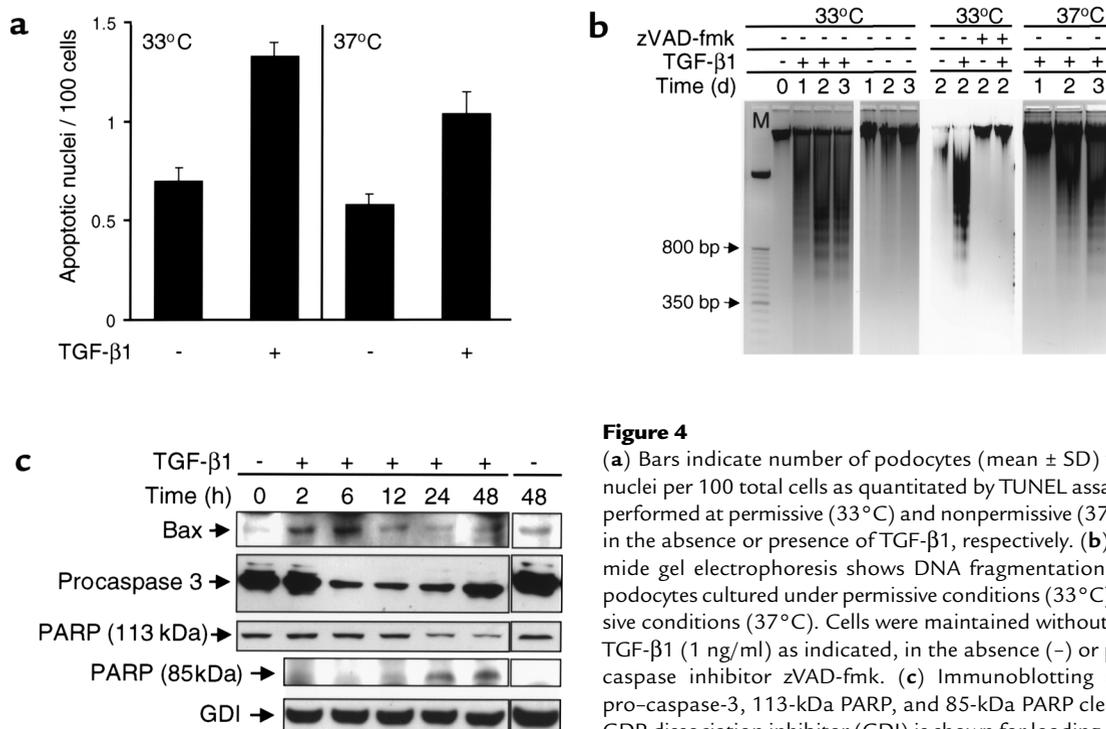
Figure 4
(**a**) Bars indicate number of podocytes (mean ± SD) with apoptotic nuclei per 100 total cells as quantitated by TUNEL assay. Analysis was performed at permissive (33°C) and nonpermissive (37°C) conditions in the absence or presence of TGF-β1, respectively. (**b**) Ethidium bromide gel electrophoresis shows DNA fragmentation (laddering) in podocytes cultured under permissive conditions (33°C) or nonpermissive conditions (37°C). Cells were maintained without (–) or with (+) TGF-β1 (1 ng/ml) as indicated, in the absence (–) or presence (+) of caspase inhibitor zVAD-fmk. (**c**) Immunoblotting detecting Bax, pro–caspase-3, 113-kDa PARP, and 85-kDa PARP cleavage product. GDP dissociation inhibitor (GDI) is shown for loading control.
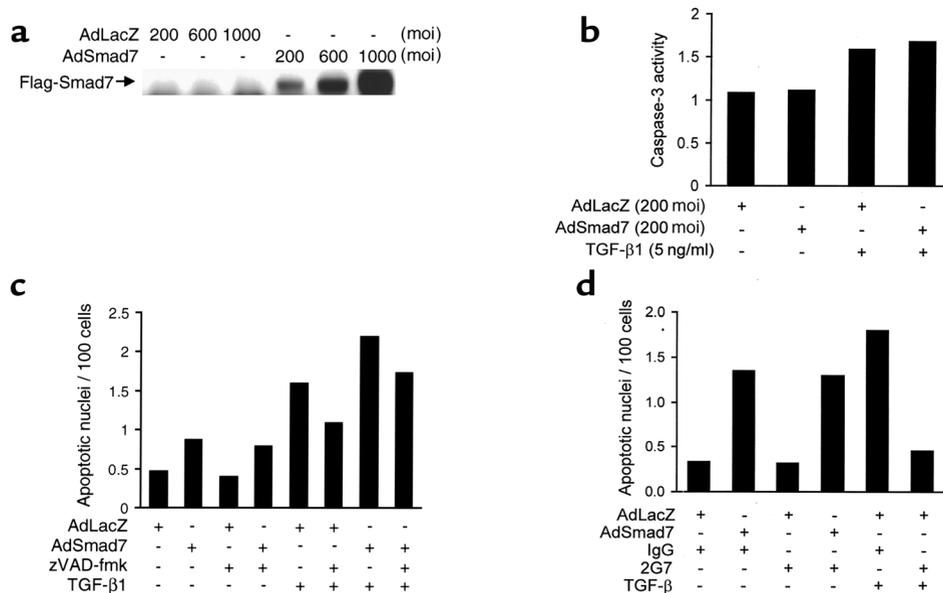
Figure 5
(**a**) Western blot demonstrates levels of Flag-Smad7 in podocytes maintained under permissive conditions. Adenoviral vectors containing either control LacZ or Flag-Smad7 cDNAs were used to infect cells at various moi's, as indicated. (**b**) Histogram shows the normalized average numbers of apoptotic cells visualized by DAPI per hpf (in 50 hpf total) from a representative experiment. Podocyte cultures were infected with AdLacZ or AdSmad7 adenoviral vectors and left untreated or treated with TGF-β1 in the absence or presence of caspase-3 inhibitor zVAD-fmk. Results were normalized for cell density. (**c**) Relative enzymatic activity of caspase-3 measured as fluorochrome release at 460 nm in infected podocytes cultured under permissive conditions in the absence (–) or presence (+) of TGF-β1. Enzyme activity is normalized to uninfected podocytes (set at 1). (**d**) Histogram shows the normalized average numbers of apoptotic cells as detected by TUNEL assay per hpf (in 50 hpf total) from a representative experiment. Podocyte cultures were infected with AdLacZ or AdSmad7 adenoviral vectors and left untreated or treated with TGF-β in the presence of control mouse immunoglobulin (IgG) or panneutralizing anti–TGF-β1 antibody (2G7). Results were normalized for total cell density.

baseline and after stimulation with TNF-α, a major activator of cytoplasmic-to-nuclear translocation of NF-κB/p65 (Figure 6c). Next, we cotransfected a NF-κB/p65–responsive luciferase reporter gene construct (14) together with either pcDNA3 control vector or pSmad7 expression vector to examine whether Smad7 expression could modulate transcriptional activity of NF-κB/p65. Both basal and TNF-α–inducible NF-κB/p65 reporter gene activity was strongly inhibited in pSmad7 cotransfected podocytes compared to pcDNA3-transfected controls (Figure 6d). TGF-β had no significant effect on NF-κB/p65 reporter gene activity (data not shown). Our data suggest that expression of Smad7 inhibits cytoplasmic-to-nuclear translocation and transcriptional activator function of the anti-apoptotic NF-κB/p65 cell survival factor in podocytes.

Discussion
Podocyte depletion has been proposed as a hallmark of both primary and secondary forms of glomerulosclerosis for many years and is now considered a central problem in progression of renal diseases (2, 3). Here we show that TGF-β1 and Smad7 induce apoptosis in podocytes through different downstream pathways, providing a novel molecular mechanism for podocyte depletion in progressive glomerulosclerosis. The following lines of evidence support our conclusion.

First, cultured podocytes undergo apoptosis when exposed to TGF-β1. Our data suggest a candidate apoptosis pathway that requires activation of p38 MAP kinase signaling and of effector caspase-3 and may involve stimulation of proapoptotic Bax protein. TGF-β has previously been shown to induce Bax gene transcription and mitochondrial translocation of Bax protein leading to release of cytochrome C from mitochondria and subsequent activation of effector caspase-3 (22). p38 MAP kinase is known to trigger apoptotic responses in cells exposed to stress or cytokines, but its downstream proapoptotic targets remain largely unknown (23). In our studies, TGF-β stimulated persistent phosphorylation of p38 between 20 minutes and 8 hours, whereas increased expression of Bax was detectable at 2–12 hours, followed by caspase-3 activation starting at 6 hours in podocytes. These kinetic profiles are consistent with a working model in which TGF-β may stimulate p38 MAP kinase signaling to induce Bax protein synthesis and mitochondrial translocation, leading to mitochondrial cytochrome C release and caspase activation (Figure 6e). Detailed studies are ongoing in our laboratory to determine the regulatory relationships and molecular determinants of mediators proposed in this model. Second, we show that increased Smad7 expression independently causes apoptosis and potentiates TGF-β–induced apoptosis in podocytes. Smad7-induced apoptosis does

not require p38 MAP kinase and caspase-3 activation. However, although TGF-β has no effect on signaling of NF-κB/p65 in podocytes (M. Schiffer and E. Böttinger, unpublished observations), Smad7 expression inhibits baseline and inducible NF-κB/p65 signaling by preventing its cytoplasmic-to-nuclear translocation. Thus we propose that Smad7 may sensitize podocytes to proapoptotic stimuli by blocking the transcriptional activation of NF-κB/p65–dependent anti-apoptotic cell survival programs (Figure 6e). Evidence for a major role of NF-κB/p65 in promoting cell survival is overwhelming, especially in the immune system, central nervous system, and liver (19). Indeed, inhibition of NF-κB/RelA can cause spontaneous apoptosis in lymphoblastoid cells (20). There is also considerable evidence suggesting an important role for NF-κB in preventing apoptosis and growth arrest induced by TGF-β in B-lymphocytes, hepatocytes, mammary epithelial cells, and certain neuronal cells (24, 25). In those reports, TGF-β was found to enhance the function of a natural cytoplasmic antagonist of NF-κB, inhibitory-kappaB (IkB). Our results demonstrate that TGF-β strongly induces synthesis of

Smad7 in podocytes and that expression of recombinant Smad7 potently inhibits transcriptional activity of NF-κB/RelA in podocytes. Our findings are consistent with recent observations indicating that Smad7 may promote apoptosis stimulated by TGF-β and serum withdrawal, as well as anoikis, in renal epithelial cells by inhibition of NF-κB (21). On the basis of these observations, we propose that Smad7 may amplify p38 MAP kinase– and caspase-dependent apoptosis induced by TGF-β through inhibition of survival factor NF-κB in podocytes (Figure 6e). Interestingly, cotransfection of Smad7 inhibited TGF-β–stimulated activation of Smad3/Smad4-dependent reporter gene constructs in podocytes (M. Schiffer and E. Böttinger, unpublished observations). Thus, we propose that Smad7 functions as a versatile regulator of separate signaling pathways and biologic responses in podocytes, including apoptosis induced by TGF-β. It will be important to understand the molecular determinants of the multifunctionality of Smad7 in podocytes that are exposed to various mediators of glomerular injury. To begin to address these challenging questions, we have generated Smad7-deficient mice as part of a collabora-
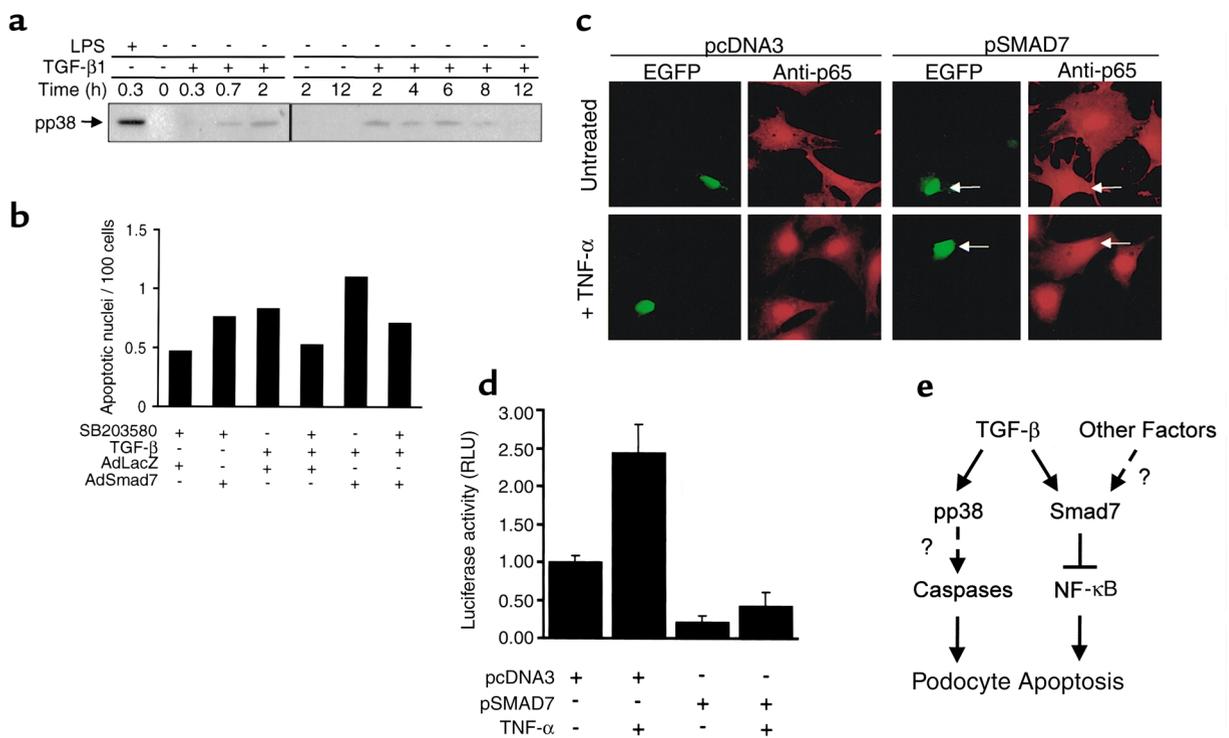
Figure 6
(**a**) Immunoblot demonstrates levels of phosphorylated p38 MAP kinase (pp38) in podocytes treated with LPS as positive control or TGF-β1 for various time intervals. (**b**) Histogram shows the normalized average numbers of apoptotic cells as detected by TUNEL assay per hpf (in 50 hpf total) from a representative experiment. Podocyte cultures were infected with AdLacZ or AdSmad7 adenoviral vectors and left untreated or treated with TGF-β in the absence or presence of p38 MAP kinase inhibitor SB203580. Results were normalized for total cell density. (**c**) Detection of the NF-κB p65-subunit (anti-p65) by indirect immunofluorescence in podocytes transiently cotransfected with green fluorescent protein expression plasmid pEGFP together with either empty control vector pcDNA3 or Smad7 expression vector pSmad7. Cells were either left untreated or treated with TNF-α for 30 minutes. Arrows indicate GFP and anti-p65 signals in pEGFP/pSmad7-cotransfected cells. (**d**) Bar graph showing normalized luciferase activity (RLU) mediated by the NF-κB–responsive reporter gene construct NF-κB-luc in podocytes cotransfected with pcDNA3 empty control or pSmad7 expression vectors. Cells were either left untreated or stimulated with TNF-α (10 ng/ml) after transfection. (**e**) Schematic demonstration of a new working model for proapoptotic signaling pathways induced by TGF-β and Smad7.

tive effort and have begun to establish Smad7-deficient podocyte cultures (W. Ju, M. Schiffer and E. Böttinger, unpublished data).

The biologic relevance of our working model is further supported by our in vivo observations using the TGF-β1 TG mouse model for progressive glomerulosclerosis. We find a strong upregulation of Smad7 in podocytes of TGF-β1 TG mice. Specifically, podocytes with morphological signs of cellular damage invariably synthesize Smad7 in our model. In a previous report, we showed upregulation of TGF-β2 and to a lesser extent TGF-β1 specifically in podocytes in TGF-β1 TG mice (26). The identity of the stimuli that are responsible for upregulation of TGF-β and/or Smad7 in podocytes in our model is unclear at present. It is possible that circulating TGF-β1, typically elevated in TGF-β1 TG mice, autoinduces local TGF-β synthesis in podocytes. Alternatively, stimuli such as mechanical stress, including stretch and pressure, and/or inflammatory mediators may induce TGF-β and/or Smad7 synthesis in podocytes, as has been shown in other systems (8).

In addition, our data demonstrate that progressive depletion of podocytes is associated with a robust increase in podocyte apoptosis that peaks at initial stages of glomerulosclerosis in kidneys from TG animals. Interestingly, a detailed morphometric study reported by Steffes and coworkers demonstrates significant podocyte depletion in patients with diabetes of only short duration (27), implying that podocyte depletion may be an initial lesion in the development of diabetic nephropathy. We intend to validate our findings in studies of chronic renal diseases in humans and mouse models.

In conclusion, we present in vitro and in vivo evidence for a new working model by which stimuli of glomerular injury converge on activation of TGF-β and Smad7 signaling in podocytes, leading to apoptosis that is cooperatively induced by TGF-β and Smad7 through separate pathways. Thus, TGF-β1 and Smad7 are novel candidate mediators to induce cellular damage and/or apoptosis in podocytes. These studies provide a novel pathomechanism for podocyte depletion as a primary irreversible lesion in progression of glomerular diseases that is consistent with the concepts of progression of glomerular diseases developed by Kriz and others (2–4). It follows from this discussion that putative therapeutic strategies, aiming at the TGF-β response system as an established key pathway in chronic renal diseases, should consider not only antifibrotic outcomes, but also cytoprotection of glomerular podocytes.

1. Ichikawa, I., and Fogo, A. 1996. Focal segmental glomerulosclerosis. *Pediatr. Nephrol.* **10**:374–391.
2. Fries, J.W., Sandstrom, D.J., Meyer, T.W., and Rennke, H.G. 1989. Glomerular hypertrophy and epithelial cell injury modulate progressive glomerulosclerosis in the rat. *Lab. Invest.* **60**:205–218.
3. Kriz, W., Gretz, N., and Lemley, K.V. 1998. Progression of glomerular diseases: is the podocyte the culprit? *Kidney Int.* **54**:687–697.
4. Kerjaschki, D. 1994. Dysfunctions of cell biological mechanisms of visceral epithelial cell (podocytes) in glomerular diseases. *Kidney Int.* **45**:300–313.
5. Border, W.A., and Noble, N.A. 1994. Transforming growth factor beta in tissue fibrosis. *N. Engl. J. Med.* **331**:1286–1292.
6. Schiffer, M., von Gersdorff, G., Bitzer, M., Susztak, K., and Bottinger, E.P. 2000. Smad proteins and transforming growth factor-beta signaling. In press. *Kidney Int.* **58**(Suppl. 77):S45–S52.
7. Nakao, A., et al. 1997. Identification of Smad7, a TGFbeta-inducible antagonist of TGF-beta signaling. *Nature.* **389**:631–635.
8. Bitzer, M., et al. 2000. A mechanism of suppression of TGF-beta/SMAD signaling by NF-kappaB/RelA. *Genes Dev.* **14**:187–197.
9. Kopp, J.B., et al. 1996. Transgenic mice with increased plasma levels of TGF-beta 1 develop progressive renal disease. *Lab. Invest.* **74**:991–1003.
10. Mundel, P., et al. 1997. Rearrangements of the cytoskeleton and cell contacts induce process formation during differentiation of conditionally immortalized mouse podocyte cell lines. *Exp. Cell Res.* **236**:248–258.
11. Mundel, P., et al. 1997. Synaptopodin: an actin-associated protein in telencephalic dendrites and renal podocytes. *J. Cell Biol.* **139**:193–204.
12. Landstrom, M., et al. 2000. Smad7 mediates apoptosis induced by transforming growth factor beta in prostatic carcinoma cells. *Curr. Biol.* **10**:535–538.
13. Fujii, M., et al. 1999. Roles of bone morphogenetic protein type I receptors and Smad proteins in osteoblast and chondroblast differentiation. *Mol. Biol. Cell* **10**:3801–3813.
14. Xu, Y., et al. 1998. NF-kappaB inactivation converts a hepatocyte cell line TNF-alpha response from proliferation to apoptosis. *Am. J. Physiol* **275**:C1058–C1066.
15. von Gersdorff, G., et al. 2000. Smad3 and Smad4 mediate transcriptional activation of the human Smad7 promoter by transforming growth factor beta. *J. Biol. Chem.* **275**:11320–11326.
16. Schrantz, N., et al. 1999. Role of caspases and possible involvement of retinoblastoma protein during TGFbeta-mediated apoptosis of human B lymphocytes. *Oncogene.* **18**:3511–3519.
17. Nicholson, D.W., et al. 1995. Identification and inhibition of the ICE/CED-3 protease necessary for mammalian apoptosis. *Nature.* **376**:37–43.
18. Arteaga, C.L., et al. 1993. Anti-transforming growth factor (TGF)-beta antibodies inhibit breast cancer cell tumorigenicity and increase mouse spleen natural killer cell activity. Implications for a possible role of tumor cell/host TGF- beta interactions in human breast cancer progression. *J. Clin. Invest.* **92**:2569–2576.
19. Barkett, M., and Gilmore, T.D. 1999. Control of apoptosis by Rel/NF-kappaB transcription factors. *Oncogene.* **18**:6910–6924.
20. Cahir-McFarland, E.D., Davidson, D.M., Schauer, S.L., Duong, J., and Kieff, E. 2000. NF-kappa B inhibition causes spontaneous apoptosis in Epstein-Barr virus-transformed lymphoblastoid cells. *Proc. Natl. Acad. Sci. USA.* **97**:6055–6060.
21. Lallemand, F., et al. 2001. Smad7 inhibits the survival nuclear factor kappaB and potentiates apoptosis in epithelial cells. *Oncogene.* **20**:879–884.
22. Teramoto, T., Kiss, A., and Thorgeirsson, S.S. 1998. Induction of p53 and Bax during TGF-beta 1 initiated apoptosis in rat liver epithelial cells. *Biochem. Biophys. Res. Commun.* **251**:56–60.
23. De Zutter, G.S., and Davis, R.J. 2001. Pro-apoptotic gene expression mediated by the p38 mitogen-activated protein kinase signal transduction pathway. *Proc. Natl. Acad. Sci. USA.* **98**:6168–6173.
24. Arsura, M., FitzGerald, M.J., Fausto, N., and Sonenshein, G.E. 1997. Nuclear factor-kappaB/Rel blocks transforming growth factor beta1-induced apoptosis of murine hepatocyte cell lines. *Cell Growth Differ.* **8**:1049–1059.
25. Kaltschmidt, B., and Kaltschmidt, C. 2001. DNA array analysis of the developing rat cerebellum: transforming growth factor-beta2 inhibits constitutively activated NF-kappaB in granule neurons. *Mech. Dev.* **101**:11–19.
26. Mozes, M.M., Bottinger, E.P., Jacot, T.A., and Kopp, J.B. 1999. Renal expression of fibrotic matrix proteins and of transforming growth factor-beta (TGF-beta) isoforms in TGF-beta transgenic mice. *J. Am. Soc. Nephrol.* **10**:271–280.
27. Steffes, M.W., Schmidt, D., McCrery, R., Basgen, J.M., and Group, I.D. 2001. Glomerular cell number in normal subjects and in type 1 diabetic patients. *Kidney Int.* **59**:2104–2113.